



# Positioning command design method for shorter distance positioning operations based on analyzed residual vibration amplitude

Kondo, Daichi  
Sato, Ryuta  
Shirase, Keiichi

---

(Citation)

Precision Engineering, 74:36-45

(Issue Date)

2022-03

(Resource Type)

journal article

(Version)

Accepted Manuscript

(Rights)

© 2021 Elsevier Inc.

This manuscript version is made available under the Creative Commons Attribution-NonCommercial-NoDerivatives 4.0 International license.

(URL)

<https://hdl.handle.net/20.500.14094/90008873>



# **Positioning Command Design Method for Shorter Distance Positioning Operations Based on Analyzed Residual Vibration Amplitude**

Daichi KONDO, Ryuta SATO, and Keiichi SHIRASE

## **Abstract**

The positioning operation of axes is essential before initiating machining operations in NC machine tools. Residual vibration following the positioning operations of the axes deteriorates the cycle time and quality of the machined parts. The purpose of this study is to establish a design method for positioning commands that reduces the residual vibration generated after positioning. Because a shorter distance positioning of several millimeters with triangular acceleration profiles is typically applied before machining, the residual vibration amplitude is formulated as a superposition of responses to step jerk inputs. By analyzing an equation that predicts the residual vibration generated by the positioning operations, the condition of the command that reduces the residual vibration is derived, and an algorithm that uniquely designs the positioning command is proposed. It is experimentally confirmed that the positioning commands designed using the proposed method can reduce residual vibrations.

**Keywords:** NC machine tools, Positioning operation, Positioning command design, Residual vibration, Suppression

## **1. Introduction**

Numerically controlled (NC) machine tools are vital to industrial applications. Because the productivity and quality of products are of utmost importance in the industry, faster and more accurate motions are required of NC machine tools. Positioning operations must be able to determine the relative position between the tool and a workpiece prior to the machining process. High-speed positioning can increase the efficiency of the entire production process. However, higher-speed positioning operations cause residual vibrations after positioning owing to increased mechanical vibration caused by larger inertial forces. If machining is performed with residual vibrations, then the quality of the machined surface deteriorates. Therefore, productivity cannot be improved because the machining process cannot commence until vibrations exist, even if higher-speed positioning is performed. Therefore, faster positioning operations without residual vibrations must be achieved.

Various studies have been performed to realize high-speed positioning operations without vibrations. In machine tools, one of the typical methods to suppress vibration is by applying a notch filter. The notch filter can reduce the gain in a specific frequency band. In other words, it can suppress vibrations

at a specific frequency [1]. It is an effective and typical method for suppressing vibrations at a specified frequency. However, the use of notch filters impairs the stability of low frequencies and adversely affects the response of the system. Machine tools generally have a natural frequency of a few tens of hertz owing to structural vibrations, which affect the relative motion between the tool and workpiece [2]. Therefore, it is difficult to prevent vibrations of several tens of hertz from occurring in machine tools using notch filters.

Another typical method for preventing vibrations is by using a Finite Impulse Response (FIR) filter. The FIR filter is applied to the position command, the time constant of the filter is set to avoid the excitation of an arbitrary vibration frequency, and a command is generated [3]. The FIR filtering approach is also an effective and typical method for suppressing vibrations by simply changing the positioning commands. However, when using a FIR filter, although the command can be designed to avoid vibrations, the positioning time must be prolonged especially for lower frequency vibrations. This poses an issue in high-speed positioning operations. Although recent discussion points of the FIR filtering approaches are to design filters for contouring control problems [4, 5], there have been no studies to achieve higher speed positioning operations using FIR filters. The input shaping method, which has been investigated to prevent the excitation of natural frequencies, poses the same problem of prolonged positioning time [6], although it can effectively suppress the residual vibration. Altintas and Khoshdarregi [7] proposed a method for designing input shaping filters to avoid residual vibrations for contour control problems. However, there has been no research on shortening the positioning time using the input shaping approach, especially for lower-frequency vibrations.

Active vibration control technology, which uses actuators to forcibly damp vibrations, has been applied to vibrations [8]. The proposed method can be effective in suppressing the vibration; however, this method must be adjusted based on the structure and machining process of the machine tool and necessitates the use of actuators and accelerometers, which are expensive and time consuming to install. Hence, Sato et al. [9] proposed a method to suppress vibrations by applying torque to vibrations without using sensors or actuators. However, this method cannot be used in all cases because the frequency of oscillation is limited, and the commands to be applied are restricted.

Herein, we propose a method for designing positioning commands that suppress residual vibrations based on jerk-limited acceleration profiles. Residual vibrations can be suppressed by designing the acceleration profile based on the analyzed vibration amplitude [10]. In a previous study [10], the authors formulated the residual vibration and found an effective combination of time parameters. However, it is impossible to design positioning commands for any positioning distance. The purpose of this study is to propose a new method for designing the optimum positioning commands based on the analysis. To achieve this purpose, in this study, the condition of a command that reduces the residual vibration is derived by analyzing an equation that predicts the residual vibration generated by positioning operations, and an algorithm that uniquely designs the positioning command is proposed.

To confirm the effectiveness of the proposed method, the residual vibrations were measured and evaluated for several distances based on positioning operations.

This paper is structured as follows. Section 2 presents the measurement and experimental method for the positioning operation. Section 3 summarizes the formulation of the jerk-limited acceleration profile and residual vibration in the case of an acceleration profile that was presented in our previous work [10]; the proposed positioning command design method is thus clearly highlighted. Sections 4 and 5 detail the proposed positioning command design method and the experimental results, respectively. Finally, the conclusions drawn from the study are provided in Section 6.

## **2. Positioning operation and measurement method**

The Z-axis of a vertical-type small machining center was adopted for testing in this study. Z-axis positioning is required prior to performing the machining operations. Each axis of the machining center was driven using an AC servomotor and a ball screw.

In this study, the relative displacement between a table and a spindle head was measured to evaluate residual vibrations after performing positioning in the Z-axis direction. The measurement setup is shown in Figure 1. The displacement was measured using a non-contact type displacement sensor (capacitive-type sensor) installed between the table and spindle. To avoid vibrations caused by the lower stiffness of the measurement setup, the displacement sensor was fixed to a JIS S45C carbon steel block that was fixed on the table. It was confirmed that the measurement setup did not affect the measurement results. In addition, during the measurement, the target position after positioning was set to zero. In other words, the deviation from the zero position was evaluated as the residual vibration.

The positioning command during the operation with shorter distances transformed into a jerk-limited waveform, as presented in Figure 2. Figure 2 shows the positioning command for a 1 mm distance generated using a conventional method obtained from the NC controller. The positional command can be recorded using the monitoring function of the controller, and the acceleration profile can be numerically calculated from the position data. As shown in the figure, the acceleration command exhibited a linear change. This implies that the jerk was limited and changed in a stepwise manner during the operation. We predicted that the machine would oscillate at the instant of jerk change.

The acceleration profile with a shorter distance positioning of a few millimeters, typically performed before machining, exhibits a triangular waveform, as shown in Figure 2. Therefore, in this study, positioning operations with shorter distances that involved the jerk-limited command were applied.

Figure 3 shows an example of the measured relative displacements of the table and spindle head, which represent the residual vibrations with the positioning command shown in Figure 2. Residual vibrations with a frequency of approximately 30 Hz were observed. It was confirmed that the relative

vibration originated from the locking mode vibration of the machine tool structure [10].

### 3. Formulation of jerk-limited acceleration profile

#### 3.1 Jerk-limited acceleration profile

The jerk-limited acceleration profile for the positioning operations are illustrated in Figure 4. The waveform can be defined by the maximum acceleration during acceleration  $A_1$ , maximum acceleration during deceleration  $A_2$ , acceleration increasing time during acceleration  $T_1$ , acceleration decreasing time during acceleration  $T_2$ , acceleration increasing time during deceleration  $T_3$ , and acceleration decreasing time during deceleration  $T_4$ .  $T_{\text{SUM}}$  is the total positioning time and can be defined as the sum of  $T_1$ ,  $T_2$ ,  $T_3$ , and  $T_4$ .

In conventional commands, the values of  $T_1$ ,  $T_2$ ,  $T_3$ , and  $T_4$  are constant, as shown in Fig. 4. A new design method for positioning commands by changing the balance of these values to prevent command-induced vibrations was proposed [10]. An important result of [10] is introduced in this section to clarify the method proposed in this study.

In the proposed method described in [10], Sato attempted to vary the parameters based on three combinations, i.e.,  $(T_1 = T_2, T_3 = T_4)$ ,  $(T_1 = T_3, T_2 = T_4)$ , and  $(T_1 = T_4, T_2 = T_3)$ . Consequently, it was revealed that the vibration of an arbitrary frequency can be suppressed by changing the parameters appropriately by setting  $T_1 = T_4$  and  $T_2 = T_3$ . Therefore, we adopted a positioning command design method by setting  $T_1 = T_4$  and  $T_2 = T_3$  in this study.

To generate commands with varying parameters  $T_1$ ,  $T_2$ ,  $T_3$ , and  $T_4$ , a relationship between the displacement and command must be formulated. This relationship can be expressed as a differential-integral relationship involving jerk, acceleration, velocity, and displacement, as shown in Fig. 5. According to Erkorkmaz and Altintas [11], the displacement can be obtained using constant jerk values  $J_1$  to  $J_4$  in each time segment from  $T_1$  to  $T_4$ , respectively. Based on the method presented in [11] for formulating a relationship between jerk and displacement, we performed the following procedure to formulate the jerk and displacement for each time-segmented command, as shown in Figure 5.

The acceleration  $a(\tau)$ , velocity  $f(\tau)$ , and displacement  $s(\tau)$  can be obtained from the jerk  $j(\tau)$ . Here,  $\tau_i$  ( $i = 1, 2, 3, 4$ ) represents the local time for the  $i$ th time segment. The jerk  $j(\tau)$  for each time segment is represented as shown in Equation (1).

$$j(\tau) = \begin{cases} J_1 & 0 \leq \tau_1 < T_1 \\ J_2 & T_1 \leq \tau_2 < T_2 \\ J_3 & T_2 \leq \tau_3 < T_3 \\ J_4 & T_3 \leq \tau_4 < T_4 \end{cases} \quad (1)$$

The acceleration for each time segment  $a(\tau)$  can be obtained from the jerk, as shown in Equation (2), where  $A_1$  is the initial value of  $\tau_2$ . This can be defined by substituting  $T_1$  with  $\tau_1$ . As shown in Figure 6, the initial value of  $a(\tau_3)$  is zero.  $A_2$ , which is the initial value of  $a(\tau_4)$ , can be defined similarly as the initial value of  $a(\tau_2)$ . Consequently, the maximum values of accelerations  $A_1$  and  $A_2$  can be

represented as shown in Equations (3) and (4), respectively.

$$a(\tau) = \begin{cases} J_1 \tau_1 \\ A_1 + J_2 \tau_2 \\ J_3 \tau_3 \\ A_2 + J_4 \tau_4 \end{cases} \quad (2)$$

$$A_1 = J_1 T_1 \quad (3)$$

$$A_2 = J_3 T_3 \quad (4)$$

The velocity  $f(\tau)$  can be obtained by integrating Equation (2) as follows:

$$f(\tau) = \begin{cases} \frac{1}{2} J_1 \tau_1^2 \\ f_1 + A_1 \tau_1 + \frac{1}{2} J_2 \tau_2^2 \\ f_2 + \frac{1}{2} J_3 \tau_3^2 \\ f_3 + A_2 \tau_4 + \frac{1}{2} J_4 \tau_4^2 \end{cases}, \quad (5)$$

where  $f_1$  to  $f_4$  are the initial values of  $f(\tau_1)$  to  $f(\tau_4)$ , respectively. The initial values can be obtained as in the case of acceleration mentioned above. The velocities  $f_1$ ,  $f_2$ , and  $f_3$  can be represented as follows:

$$f_1 = \frac{1}{2} J_1 T_1^2 \quad (6)$$

$$f_2 = f_1 + A_1 T_2 + \frac{1}{2} J_2 T_2^2 \quad (7)$$

$$f_3 = f_2 + \frac{1}{2} J_2 T_3^2 \quad (8)$$

Similarly, displacement  $s(\tau)$  can be represented as Equation (9), where the initial values  $s_1$ ,  $s_2$ , and  $s_3$  are as shown in Equations (10) to (12), respectively.

$$s(\tau) = \begin{cases} \frac{1}{6} J_1 \tau_1^3 \\ s_1 + f_1 \tau_2 + \frac{1}{2} A_1 \tau_2^2 + \frac{1}{6} J_2 \tau_2^3 \\ s_2 + f_2 \tau_3 + \frac{1}{6} J_3 \tau_3^3 \\ s_3 + f_3 \tau_4 + \frac{1}{2} A_2 \tau_4^2 + \frac{1}{6} J_4 \tau_4^3 \end{cases} \quad (9)$$

$$s_1 = \frac{1}{6} J_1 T_1^3 \quad (10)$$

$$s_2 = s_1 + f_1 T_2 + \frac{1}{2} A_1 T_2^2 + \frac{1}{6} J_2 T_2^3 \quad (11)$$

$$s_3 = s_2 + f_2 T_3 + \frac{1}{6} J_3 T_3^3 \quad (12)$$

In addition, the positioning distance  $L$  can be represented by substituting  $T_4$  to  $\tau_4$  in  $s(\tau_4)$ , as in Equation (13).

$$L = s_3 + f_3 T_4 + \frac{1}{2} A_2 T_4^2 + \frac{1}{6} J_4 T_4^3 \quad (13)$$

By incorporating constraints  $T_1 = T_4$  and  $T_2 = T_3$  to Equation (13), the latter can be transformed into an equation with fewer variables. Considering the abovementioned constraints and the velocity at displacement  $L$  after positioning, the maximum acceleration  $A_2$  is equal to  $-A_1$ . In addition, jerk  $J_1$  should be equal to  $J_4$ , and  $J_2$  should be equal to  $J_3$ . By substituting the constraint in Equation (13), the following can be obtained:

$$L = \frac{1}{3} A_1 T_1^2 + A_1 T_1 T_2 + \frac{2}{3} A_1 T_2^2 \quad (14)$$

The ratio of  $T_2$  to  $T_1$  is defined as  $R$ , as shown in Equation (15). Based on this definition,  $T_2$  can be represented as a function of  $T_1$  and  $T_{SUM}$ , as shown in Equation (16). In addition, the ratio  $R$  can be represented as shown in Equation (17).

$$T_2 = R T_1 \quad (15)$$

$$T_2 = \frac{T_{SUM} - T_1}{2} \quad (16)$$

$$R = \frac{T_{SUM} - 2T_1}{2T_1} \quad (17)$$

Subsequently,  $L$  can be represented as shown in Equation (18) by substituting Equations (15), (16), and (17) into Equation (14).

$$L = \frac{1}{6} (2R + 1) T_{SUM} A_1 T_1 \quad (18)$$

Equation (18) can be transformed into Equation (19) because acceleration  $A_1$  is a product of  $J_1$  and  $T_1$ . As shown in Equation (19),  $J_1$  can be defined based on three parameters:  $T_{SUM}$ ,  $T_1$ , and  $L$ . Furthermore,  $T_2$  and  $J_2$  can be defined as  $T_4$  and  $J_4$ , respectively, based on the defined constraint.

$$J_1 = \frac{6L}{T_1^2 T_{SUM} (2R + 1)} \quad (19)$$

### 3.2 Formulation of generated residual vibration amplitude

To formulate an expression for the amplitude of the oscillating vibrations, a standard second-order transfer function, as shown in Equation (20), was assumed in this study. The response to the stepwise jerk change  $y(t)$  can be represented as the sum of the step responses, as shown in Equation (21).

$$G(s) = \frac{\omega_n^2}{s^2 + 2\zeta\omega_n s + \omega_n^2} \quad (20)$$

$$\begin{aligned}
y(t) = \frac{e^{-\zeta\omega_n t}}{\sqrt{1-\zeta^2}} \{ & -J_1 e^{-\zeta\omega_n(T_1+T_2)} \sin(\omega_d(t+T_1+T_2)+\varphi) \\
& -(-J_1+J_2)e^{-\zeta\omega_n T_2} \sin(\omega_d(t+T_2)+\varphi) - (-J_2+J_3) \sin(\omega_d t+\varphi) \\
& -(J_3+J_4)e^{\zeta\omega_n T_3} \sin(\omega_d(t-T_3)+\varphi) - J_4 e^{\zeta\omega_n(T_3+T_4)} \sin(\omega_d(t-T_3-T_4)+\varphi) \},
\end{aligned} \quad (21)$$

where  $\omega_d$  and  $\varphi$  are represented by Equations (22) and (23), respectively.

$$\omega_d = \sqrt{1-\zeta^2}\omega_n \quad (22)$$

$$\varphi = \tan^{-1} \frac{\sqrt{1-\zeta^2}}{\zeta} \quad (23)$$

To simplify the results, the damping ratio  $\zeta$  was assumed to be zero in this study. Equation (21) can be simplified to Equation (24) under the assumption that,

$$\begin{aligned}
y(t) = \frac{1}{\omega_n} \{ & J_1 \sin \omega_n(t+T_1+T_2) - (-J_1+J_2) \sin \omega_n(t+T_2) - (-J_1+J_3) \sin \omega_n t \\
& -(-J_3+J_4) \sin \omega_n(t-T_3) + J_4 \sin \omega_n(t-T_3-T_4) \}
\end{aligned} \quad (24)$$

Using the constraint in Equation (25) and considering the coefficient of the response equation shown in Equation (24), the vibration amplitude  $x$  can be expressed as shown in Equation (26).

$$J_2 = -\frac{1}{R}J_1 \quad (25)$$

$$x = \frac{2J_1}{\omega_n} \left\{ \left(1 + \frac{1}{R}\right) \sin \omega_n R T_1 - \sin \omega_n \frac{T_{SUM}}{2} \right\} \quad (26)$$

Based on the relationship between  $J_1$  and  $L$  from Equation (19), the following equation expressing the relationship among  $T_1$ ,  $T_{SUM}$ , and  $\omega_n$  is obtained:

$$x = \frac{12L}{T_1^2 T_{SUM} \omega_n (2R+1)} \left\{ \left(1 + \frac{1}{R}\right) \sin \omega_n R T_1 - \sin \omega_n \frac{T_{SUM}}{2} \right\} \quad (27)$$

Equation (27) represents the acceleration amplitude of the residual vibration because the solution was obtained as a response to the acceleration command.

#### 4. Analysis of residual vibration changes

##### 4.1 Analytical optimum solution

It has already been clarified that the residual vibration amplitude can be represented as an amplitude map for a specified  $\omega_n$  [10]. According to a previous study [10], it is possible to choose  $T_1$ ,



which can minimize the residual vibration for a specified  $T_{\text{SUM}}$  and  $\omega_n$ . However, it is impossible to design positioning commands for any positioning distance. A method for designing an optimum positioning command that can minimize the residual vibration for a specified  $T_{\text{SUM}}$ ,  $\omega_n$ , and positioning distance is proposed in this study based on the analyzed amplitude solution.

Based on the equations presented in the previous section, the conditions that can eliminate residual vibrations were analyzed. Subsequently, Equation (28) was obtained by substituting Equation (17) into Equation (27).

$$x = \frac{12L}{T_1 T_{\text{SUM}} \omega_n (T_{\text{SUM}} - T_1)} \left\{ \left( \frac{T_{\text{SUM}}}{T_{\text{SUM}} - 2T_1} \right) \sin \omega_n \left( \frac{T_{\text{SUM}} - 2T_1}{2} \right) - \sin \left( \frac{\omega_n T_{\text{SUM}}}{2} \right) \right\} \quad (28)$$

In Equation (28),  $T_1$  and  $T_{\text{SUM}}$  are variables that can be used to derive the vibration amplitude for an arbitrary position distance  $L$  and angular frequency  $\omega_n$ . The generated vibration amplitude becomes zero theoretically when the solution of the equation is zero. By specifying the variables in the equation, such as the total positioning time  $T_{\text{SUM}}$  to be generated, and based on  $L$  and  $\omega_n$ , Equation (28) can be set to 0, as shown in Equation (29). Therefore,  $T_1$ , which satisfies the equation, can be obtained under the specified settings of  $T_{\text{SUM}}$ ,  $L$ , and  $\omega_n$ . At this time, because the variable  $T_1$  can be determined, all the components necessary for generating a command can be derived from Equations (16) and (18); this implies that the command whose vibration amplitude is zero theoretically can be determined uniquely.

$$0 = \frac{12L}{T_1 T_{\text{SUM}} \omega_n (T_{\text{SUM}} - T_1)} \left\{ \left( \frac{T_{\text{SUM}}}{T_{\text{SUM}} - 2T_1} \right) \sin \omega_n \left( \frac{T_{\text{SUM}} - 2T_1}{2} \right) - \sin \left( \frac{\omega_n T_{\text{SUM}}}{2} \right) \right\} \quad (29)$$

To derive the solutions, the equation is decomposed into component  $A$ , which determines the zero solution in Equation (29), and coefficient component  $B$ . By this decomposition, the calculation of Equation (28) can be reduced to the calculation of Equation (32). According to the dimensional analysis, note that component  $A$  does not have any physical dimension, although component  $B$  has a physical acceleration dimension,  $\text{m/s}^2$ .

However, the equation is difficult to solve directly even after it has been decomposed. Therefore, in this study, the optimal value of  $T_1$  was obtained numerically by substituting  $T_1$  into Equation (30).

$$A = \left\{ \left( \frac{T_{\text{SUM}}}{T_{\text{SUM}} - 2T_1} \right) \sin \omega_n \left( \frac{T_{\text{SUM}} - 2T_1}{2} \right) - \sin \left( \frac{\omega_n T_{\text{SUM}}}{2} \right) \right\} \quad (30)$$

$$B = \frac{12L}{T_1 T_{\text{SUM}} \omega_n (T_{\text{SUM}} - T_1)} \quad (31)$$

$$0 = \left\{ \left( \frac{T_{\text{SUM}}}{T_{\text{SUM}} - 2T_1} \right) \sin \omega_n \left( \frac{T_{\text{SUM}} - 2T_1}{2} \right) - \sin \left( \frac{\omega_n T_{\text{SUM}}}{2} \right) \right\} \quad (32)$$

Figure 7 (a) shows the results calculated using Equation (30) when  $\omega_n = 60\pi$  (30 Hz) and  $T_{\text{SUM}} = 0.07$  s. The horizontal and vertical axes are represented by  $T_1$  and  $A$ , respectively. In this study, a commercial NC machine tool was used in the experiments. Conventional positioning commands are generated by the conventional positioning command design method based on the acceleration and velocity limitations implemented in the controller. Because the effectiveness of the proposed command design method is evaluated by comparing it with the conventional design method, the authors use the total positioning time  $T_{\text{SUM}}$  of the command designed by the conventional algorithm for each positioning distance  $L$ . Total positioning time  $T_{\text{SUM}}$  becomes 0.07 s by the conventional positioning command design method implemented in the controller with a positioning distance  $L$  of 6 mm.

As shown in Figure 7 (a), the sign of  $A$  is reversed in the range  $0 < T_1 < T_{\text{SUM}}/2$  when  $\omega_n = 60\pi$  and  $T_{\text{SUM}} = 0.07$  s. This implies that a solution exists with  $A = 0$ . In this case, the vibration amplitude becomes zero regardless of the value of  $B$ , and the optimal  $T_1$  can be obtained uniquely. Therefore, the command that suppresses the residual vibration with a frequency of 30 Hz when  $T_{\text{SUM}} = 0.07$  s can be uniquely designed based on  $T_1 = T_4$  and  $T_2 = T_3$  from the obtained  $T_1$  and the total positioning time  $T_{\text{SUM}}$ .

Figure 7 (b) shows the result calculated using Equation (30) with  $\omega_n = 60\pi$  (30 Hz) and  $T_{\text{SUM}} = 0.04$  s. Total positioning time  $T_{\text{SUM}}$  becomes 0.04 s by the conventional positioning command design method implemented in the controller with a positioning distance  $L$  of 1 mm. As shown in Figure 7 (b), the sign of  $A$  is not reversed within the range  $0 < T_1 < T_{\text{SUM}}/2$ . This implies that no solution exists with  $A = 0$ . Consequently, the optimal  $T_1$  that minimizes the amplitude  $x$  cannot be obtained, and the command for suppressing the residual vibration cannot be uniquely designed based on only Equation (30).

#### 4.2 Non-existence of analytical solution

It was founded that there may be no solution for  $T_1$  within the available range of  $T_1$  depending on the conditions of the specified angular frequency  $\omega_n$  and total positioning time  $T_{\text{SUM}}$ . The function  $A$  in Equation (30) contains sinusoidal functions, and  $A$  changes periodically as a function of  $T_1$ . Therefore, it can be speculated that the condition that allows a solution for  $T_1$  within the range  $0 < T_1 < T_{\text{SUM}}/2$  might be the condition with a shorter sine wave period and a longer  $T_{\text{SUM}}$ . In other words, the available analytical solution can appear in a higher  $\omega_n$  and a longer  $T_{\text{SUM}}$ .

For the 30 Hz vibration, the range of  $T_{\text{SUM}}$  that cannot yield a solution for  $T_1$  within the range  $0 < T_1 < T_{\text{SUM}}/2$  must be investigated. After performing a comprehensive computational investigation of

the equation, it was discovered the range  $0 < T_{\text{SUM}} < 0.0478$  could not yield a solution. This indicates that if  $T_{\text{SUM}}$  is longer than 0.0478, then a solution for  $T_1$  exists that can achieve  $A = 0$ , and the optimum positional command can be designed uniquely. However, it remains impossible to design the positional command under the condition  $0 < T_{\text{SUM}} < 0.0478$ .

To achieve an optimal command design without the solution of  $T_1$ , the behavior of the vibration amplitude  $x$  in Equation (28) was investigated within the range  $0 < T_{\text{SUM}} < 0.0478$ . Figure 8 shows the relationship between  $T_1$  and the vibration amplitude  $x$ . An example of the relationship between  $T_1$  and  $x$  when  $\omega_n = 60\pi$ ,  $T_{\text{SUM}} = 0.04$  s, and  $L = 0.001$  m is depicted. According to the figure, the vibration amplitude change gradient is positive when  $T_1$  is smaller than 0.02 s in this case. This means that the  $T_1$  should be as small as possible to suppress the residual vibrations because  $T_1$  cannot be larger than 0.02 s, the half value of  $T_{\text{SUM}}$  (0.04 s). Therefore, it was expected that  $T_1$  can be set to the minimum possible value in the case where the analytical solution does not exist to minimize the residual vibration.

To confirm that the strategy can be applied in any case, the relationship between  $T_{\text{SUM}}$ ,  $T_1$ , and the gradient of the amplitude was investigated. The gradient of the vibration amplitude  $x$  can be obtained as the first derivative of the analyzed vibration amplitude  $x$ , as shown in Equation (33).

$$x' = \frac{12L}{T_1 T_{\text{SUM}} \omega_n (T_1 - T_{\text{SUM}})} \left\{ \begin{aligned} & \frac{2T_1 - T_{\text{SUM}}}{T_1(T_1 - T_{\text{SUM}})} \frac{T_{\text{SUM}}}{T_{\text{SUM}} - 2T_1} \sin\left(\frac{\omega_n(T_{\text{SUM}} - 2T_1)}{2}\right) \\ & - \frac{2T_{\text{SUM}}}{(T_{\text{SUM}} - 2T_1)^2} \sin\left(\frac{\omega_n(T_{\text{SUM}} - 2T_1)}{2}\right) \\ & + \frac{\omega_n T_{\text{SUM}}}{T_{\text{SUM}} - 2T_1} \cos\left(\frac{\omega_n(T_{\text{SUM}} - 2T_1)}{2}\right) - \frac{2T_1 - T_{\text{SUM}}}{T_1(T_1 - T_{\text{SUM}})} \frac{\sin \omega_n T_{\text{SUM}}}{2} \end{aligned} \right\} \quad (33)$$

To determine the behavior of  $x$  for the condition without a solution ( $0 < T_{\text{SUM}} < 0.0478$ ), the sign of the gradient  $x'$  was numerically investigated because the relationships are not easily imagined from Equation (33). An  $L$  of 1 mm was assumed, which did not affect the sign of the slope. The signs of the slope were calculated by numerically substituting variables  $T_1$  and  $T_{\text{SUM}}$ , and the results are shown in Figure 9.

As presented in Figure 9, the slope  $x'$  of the vibration amplitude  $x$  is always positive in the range  $0 < T_{\text{SUM}} < 0.0478$ ; meanwhile, in the range that cannot yield a solution, the slopes of the vibration amplitude  $x$  are always positive. In other words, in the range  $0 < T_{\text{SUM}} < 0.0478$  for a 30 Hz vibration, the vibration amplitude  $x$  always becomes smaller with smaller  $T_1$ .

In addition, to obtain the optimum  $T_1$ , the value of  $x$  at a  $T_1$  of approximately zero must be determined. Therefore, the starting value of the vibration amplitude  $x$  with respect to  $T_1$  must be obtained, i.e., the positive and negative amplitudes of  $x$  at  $T_1 = 0$ .

The positive and negative values of  $x$  at  $T_1 = 0$  can be explained as follows: The vibration amplitude  $x$  is expressed as shown in Equation (29), and its value at  $T_1 = 0$  must be obtained. However, the

vibration amplitude  $x$  shown in Equation (29) cannot be defined when  $T_1 = 0$ . Therefore, L'Hopital's theorem was applied to obtain the value of  $x$  that converges as  $T_1 \rightarrow 0$ . By applying L'Hopital's theorem to Equation (29), the result can be expressed as shown in Equation (34). Because the common factor in Equation (34) does not determine the values, the term required to determine the values is defined as  $C$ , which is expressed as shown in Equation (35).

$$\lim_{T_1 \rightarrow 0} x = \frac{12L}{T_{\text{SUM}}^3 \omega_n} \left\{ 2 \sin \left( \frac{\omega_n T_{\text{SUM}}}{2} \right) - \omega_n T_{\text{SUM}} \cos \left( \frac{\omega_n T_{\text{SUM}}}{2} \right) \right\} \quad (34)$$

$$C = \left\{ 2 \sin \left( \frac{\omega_n T_{\text{SUM}}}{2} \right) - \omega_n T_{\text{SUM}} \cos \left( \frac{\omega_n T_{\text{SUM}}}{2} \right) \right\} \quad (35)$$

Based on Equation (35), one can evaluate the vibration amplitude changes when  $T_1 \rightarrow 0$  under the assumption of  $\omega_n = 60\pi$ , which represents the 30 Hz vibration.  $C$  can be represented as a function of  $T_{\text{SUM}}$ , as shown in Figure 10. As presented in Figure 10,  $C$  is always positive within the range  $0 < T_{\text{SUM}} < 0.0478$ , and this range cannot yield a solution for  $T_1$  with  $A = 0$ . In other words, the value of  $x$  that converges when  $T_1 \rightarrow 0$  is always positive in this range.

Therefore, the change in the vibration amplitude  $x$  is always positive with respect to the change in  $T_1$  in the range  $0 < T_{\text{SUM}} < 0.0478$ . This implies that the residual vibration amplitude  $x$  increases with respect to  $T_1$  in the range  $0 < T_{\text{SUM}} < 0.0478$ . Therefore, it can be concluded that the minimum  $T_1$  should be applied to minimize the vibration amplitude when a solution of  $A = 0$  cannot be obtained.

## 5. Positional command design algorithm based on analyzed vibration amplitude

### 5.1 Positional command design algorithm

A positional command design method based on the abovementioned investigation is proposed herein. The proposed method can be used to design a positional command that can minimize the residual vibration for each  $\omega_n$  and  $T_{\text{SUM}}$ .

The proposed algorithm is illustrated in Fig. 11. In the proposed algorithm,  $\omega_n$  and  $T_{\text{SUM}}$  were first set. To obtain the solution of  $T_1$  that yields a solution of  $A = 0$ , Equation (30) was calculated by changing  $T_1$ . The minimum value of  $T_1$  was  $T_c$ , the minimum command setting time interval of the controller was 0.001 s (in this study), and the maximum value of  $T_1$  was  $T_{\text{SUM}}/2$ . If the sign of the amplitude parameter  $A$  is changed in the available range of  $T_1$ , then a zero-amplitude solution exists. In this case, the value of  $T_1$  is recorded as the optimum solution, and the positioning command can be uniquely designed based on the obtained  $T_1$ . By contrast, if the sign of  $A$  does not reverse within the available range of  $T_1$ , then the shorter  $T_1$  obtained will result in a smaller vibration amplitude. The minimum value of  $T_1$  can be set to  $T_c$ . Because the minimum value of  $T_1$  is  $T_c$ , if the sign of  $A$  does not

reverse within the available range of  $T_1$ , then  $T_1$  is set as  $T_c$ , and the positioning command can be designed based on the obtained  $T_1$ .

## 5.2 Designed positional commands and experimental results

Figure 12 shows the time vs.  $L$  plots for  $T_{SUM}$ ,  $T_1$  in the conventional profile ( $T_1 = T_{SUM}/4$ ), and  $T_1$  designed using the proposed algorithm.  $T_{SUM}$  depended on  $L$  (1–6 mm) owing to acceleration and velocity limitations. The relationships between the  $T_{SUM}$  and  $T_1$  values obtained from the conventional and proposed algorithms are shown in Figure 12.

As shown in Figure 12, for shorter  $L$  (1 and 2 mm), the designed  $T_1$  became  $T_c$ . This implies that the algorithm could not obtain the theoretical optimum value owing to the shorter  $T_{SUM}$ . Additionally, the designed optimum  $T_1$  depended on  $L$  of 3, 4, 5, and 6 mm. This implies that the optimum solution that can yield  $A = 0$  existed in these cases.

From a practical point of view, the user does not have to calculate the optimum  $T_1$  for each positioning distance because the optimum value changes linearly in the existing solution. The method can be implemented into the controller as a table of several optimum values depending on the total positioning time  $T_{SUM}$ , and the optimum  $T_1$  can be obtained from the table by using interpolation techniques.

To confirm the effectiveness of the proposed algorithm, experiments were performed using the conventional and designed positioning commands. The experimental results for  $L = 1$  and 3 mm are shown in Figures 13 and 14, respectively. Figure 13 shows the results in the case where an analytical solution does not exist (case discussed in Section 4.2), and Figure 14 shows the results in the case where an analytical solution exists (case discussed in Section 4.1). In both, (a) is the acceleration command, (b) the measured residual vibration, and (c) the frequency analysis results of the residual vibration. As shown by the residual vibrations in figures (b), the residual vibrations of the proposed positioning commands were smaller than those of the conventional ones for both values of  $L$ . Additionally, the frequency analysis results presented in Figure (c) show that the 30 Hz vibrations were suppressed significantly by the proposed method.

According to the figures, in addition, the results shown in Figure 14 have a better vibration suppression effect than the results shown in Figure 13, because Figure 14 shows the results in the case where an analytical solution exists. Unfortunately, it was impossible to completely eliminate the residual vibration, even though the optimum analytical solution could be found. Although the analytical solutions are obtained based on a simple 2nd order transfer function, the actual residual vibration is influenced by several vibration modes. The authors are planning to develop a positioning command design method for several vibration frequencies.

Because the purpose of this command is to suppress the vibration frequency of 30 Hz, other frequencies may increase compared with the case involving the conventional command. However,

because the effects of other frequencies were less prominent than that of the 30 Hz vibration, the proposed positioning command design method can effectively suppress the residual vibrations after positioning without changing  $T_{\text{SUM}}$ .

It is a fact that the jerk of the positioning commands designed by the proposed method is larger than that of conventional commands. However, the residual vibrations were reduced by the proposed method. This is a significant and interesting point for the proposed method. The axis cannot follow the commanded jerk change because the position and velocity feedback control acts as a low-pass filter to the positioning command. It is also not necessary to follow commands. The important point is the oscillated vibration owing to the jerk changes in the command. The analytical solution indicates that the vibrations oscillated by each jerk change can be canceled out when the timing of the jerk change is properly designed.

## 6. Conclusion

An effective method for suppressing residual vibrations without requiring additional sensors or actuators and without changing the positioning time was proposed herein. Specifically, an appropriate design for a jerk-limited acceleration profile during acceleration and deceleration was proposed. To design an appropriate jerk profile, an algorithm was proposed to design a positional command based on the analysis of residual vibrations. By analyzing an equation that predicts the residual vibration generated by positioning operations, the condition of a command that reduces the residual vibration was derived, and an algorithm that uniquely designs the positioning command was proposed. To confirm the effectiveness of the proposed method, the residual vibrations were measured and evaluated for several distances of the positioning operations. The conclusions of this study can be summarized as follows:

- (1) The vibration amplitude can be expressed as a function of  $T_{\text{SUM}}$ ,  $T_1$ ,  $\omega_n$ , and  $L$  under constraints  $T_1 = T_4$  and  $T_2 = T_3$ .
- (2) By solving an equation that represents the vibration amplitude, the optimal  $T_1$  that can suppress vibrations for the specified  $T_{\text{SUM}}$  can be obtained as a unique solution of the equation under the constraint that  $T_{\text{SUM}}$  is relatively longer than the vibration period.
- (3) In the case where the equation could not yield a unique solution, it was confirmed that a shorter  $T_1$  resulted in a smaller vibration. The optimum  $T_1$  that can suppress vibrations can be regarded as the minimum command setting time interval of the controller  $T_c$ .
- (4) The positioning command design algorithm, which can reduce residual vibrations, can be realized via analysis. It was confirmed that the proposed positioning commands designed by the algorithm suppressed residual vibrations significant even when  $L$  was changed.

The proposed positioning command design algorithm can be used to design a novel positioning command that can reduce residual vibrations for shorter distance positioning operations. The proposed positioning command can effectively suppress residual vibrations without requiring additional sensors or actuators, as well as without changing  $T_{SUM}$ . In the future, the authors will attempt to develop a method to reduce  $T_{SUM}$  under the constraint of the allowable vibration amplitude using the proposed positioning command design approach. The authors will also try to establish a general positioning command design theorem and explanations, which can become a new normal theory that can be applied in industry.

## Reference

- [1] Kuo, B.C., Frequency-domain design of control systems, Automatic Control Systems, 6th ed.; Prentice Hall International: New Jersey, USA, 1991, 664-720.
- [2] Sato, R., Tashiro, G., Shirase, K., Analysis of the coupled vibration between feed drive systems and machine tool structure, *Int. J. Autom. Technol.*, 9, (2015), 689-697.
- [3] Chen, C.-S., Lee, A.-C., Design of acceleration/deceleration profiles in motion control based on digital FIR filters, *Int. J. Mach. Tool. Manuf.*, 38, (1998), 799-825.
- [4] Tajima, S., Sencer, B., Shamoto, E., Accurate interpolation of machining tool-paths based on FIR filtering, *Precis. Eng.*, 52, (2018), 332-344.
- [5] Sencer, B., Ishizaki, K., Shamoto, E., High speed cornering strategy with confined contour error and vibration suppression for CNC machine tools, *CIRP Ann. Manuf. Technol.*, 64, (2015), 369-372.
- [6] Singer, N.C., Seering, W.P., Preshaping command inputs to reduce system vibration, *Meas. Control*, 112, (1990), 76-82.
- [7] Altintas, Y., Khoshdarregi, M.R., Contour error control of CNC machine tools with vibration avoidance, *CIRP Ann.*, 61, (2012), 335-338.
- [8] Zaeh, M.F., Kleinwort, R., Fagerer, P., Altintas, Y., Automatic tuning of active vibration control systems using inertial actuators, *CIRP Ann. Manuf. Technol.*, 66, (2017), 365-368.
- [9] Sato, R., Hayashi, H., Shirase, K., Active vibration suppression of NC machine tools for high-speed contouring motions, *J. Adv. Mech. Des. Syst. Manuf.*, 14, (2020), No.19-00274, JAMDSM0005-JAMDSM0005.
- [10] Sato, R., Shirase, K., Analytical time constant design for jerk-limited acceleration profiles to minimize residual vibration after positioning operation in NC machine tools, *Precis. Eng.*, 71, (2021), 47-56.
- [11] Erkorkmaz, K., Altintas, Y., High speed CNC system design. Part I: jerk limited trajectory generation and quantic spline interpolation, *Int. J. Mach. Tool. Manuf.*, 41, (2001), 1323-1345.

Figures:

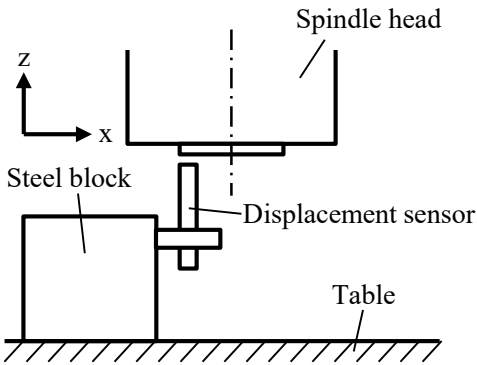
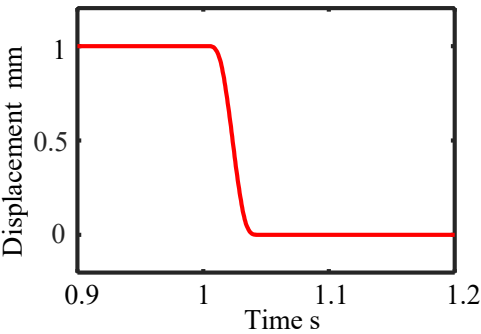
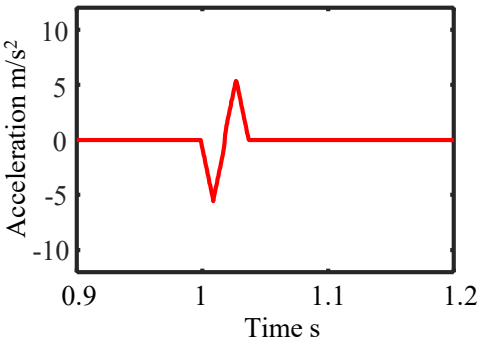


Figure 1: Measurement setup



(a) Positional command



(b) Acceleration command

Figure 2: Positional and acceleration command



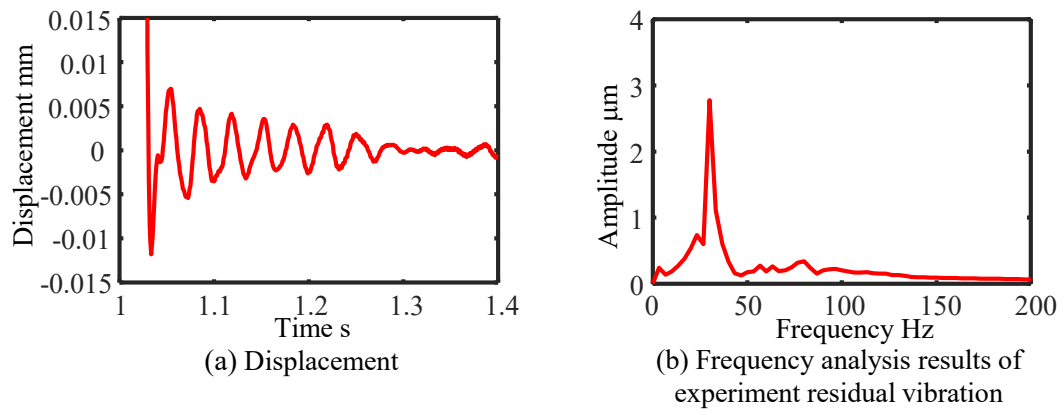


Figure 3: Experiment results based on conventional acceleration command

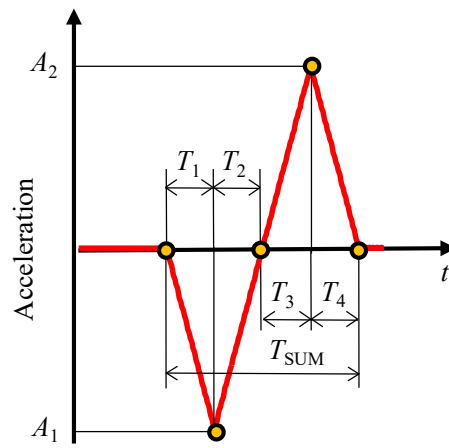


Figure 4: Jerk-limited acceleration profile for positioning operations

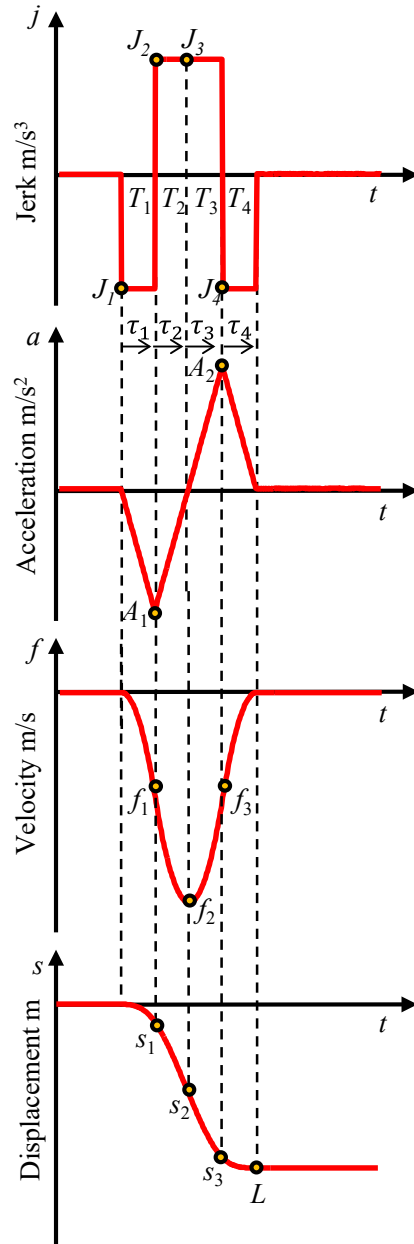


Figure 5: Jerk, acceleration, velocity, and displacement of positioning motions

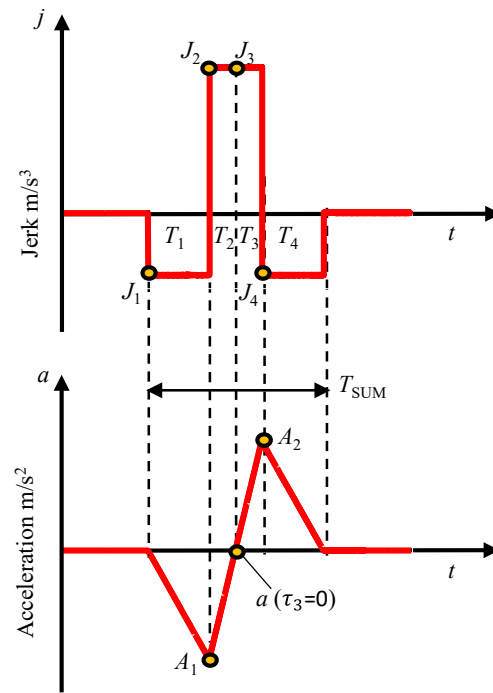
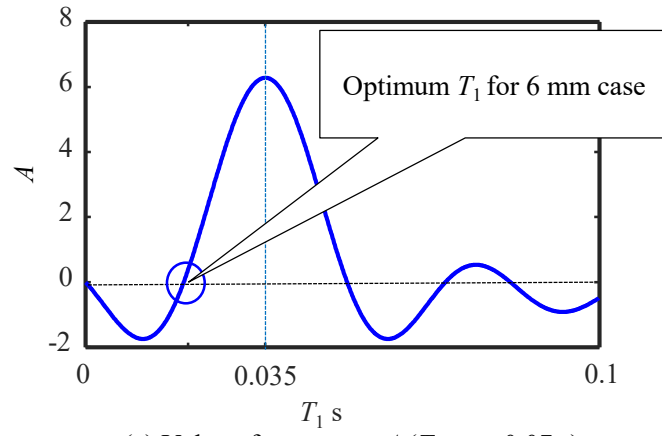
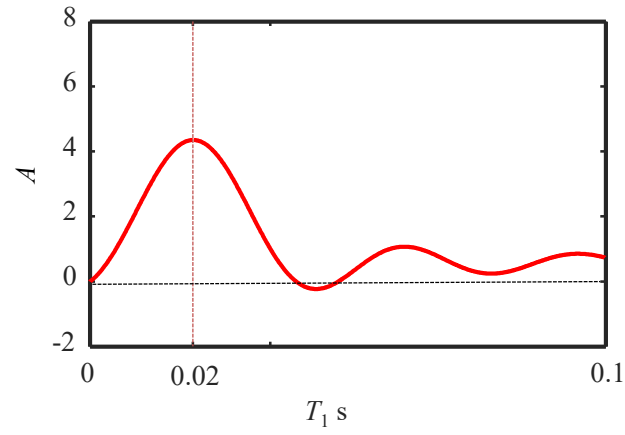


Figure 6: Jerk and acceleration of proposed positioning commands



(a) Value of parameter  $A$  ( $T_{\text{SUM}} = 0.07$  s)



(b) Value of parameter  $A$  ( $T_{\text{SUM}} = 0.04$  s)

Figure 7: Relationship between  $T_1$  and amplitude parameter  $A$

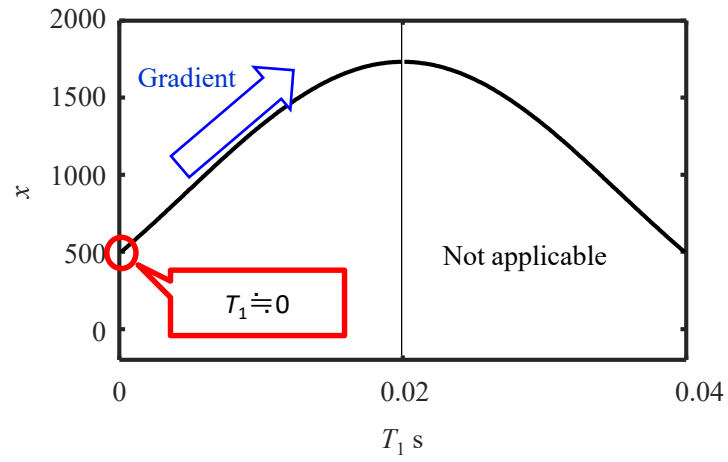


Figure 8: Relationship between  $T_1$  and vibration amplitude  
 $(\omega_n = 60\pi, T_{\text{SUM}} = 0.04 \text{ s}, L = 0.001)$

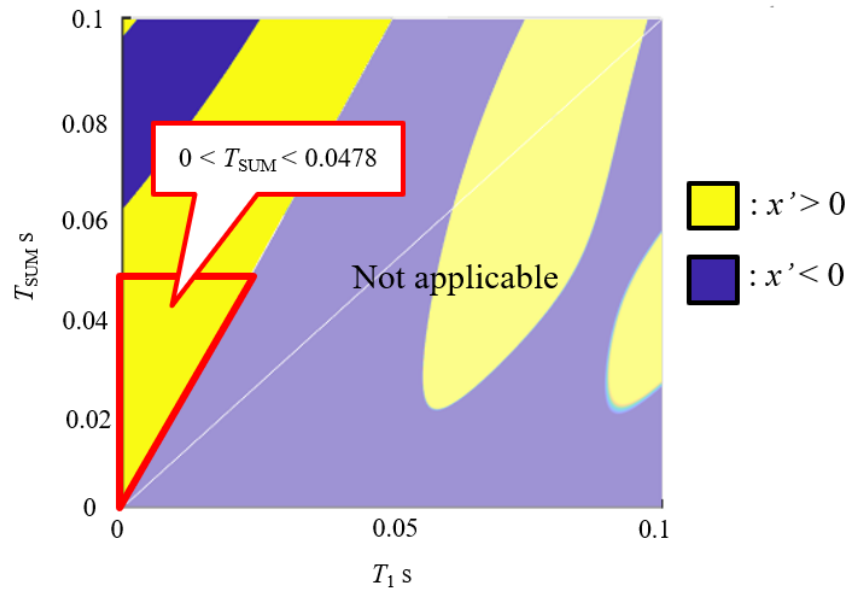


Figure 9: Evaluated gradient of vibration amplitude changes

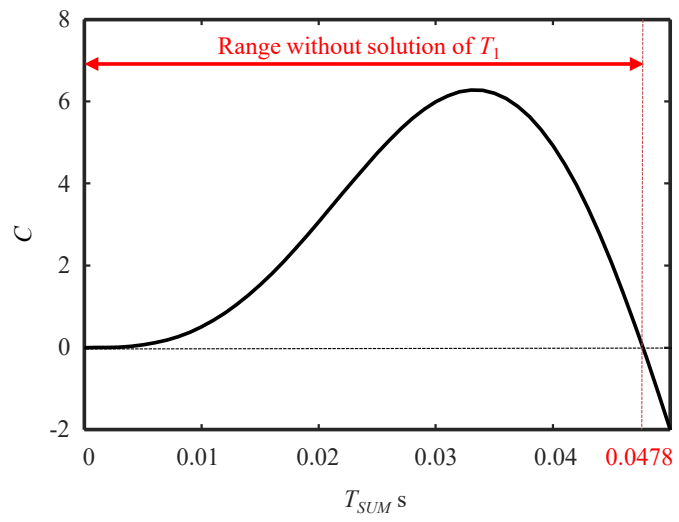


Figure 10: Relationship between  $T_{SUM}$  and  $C$

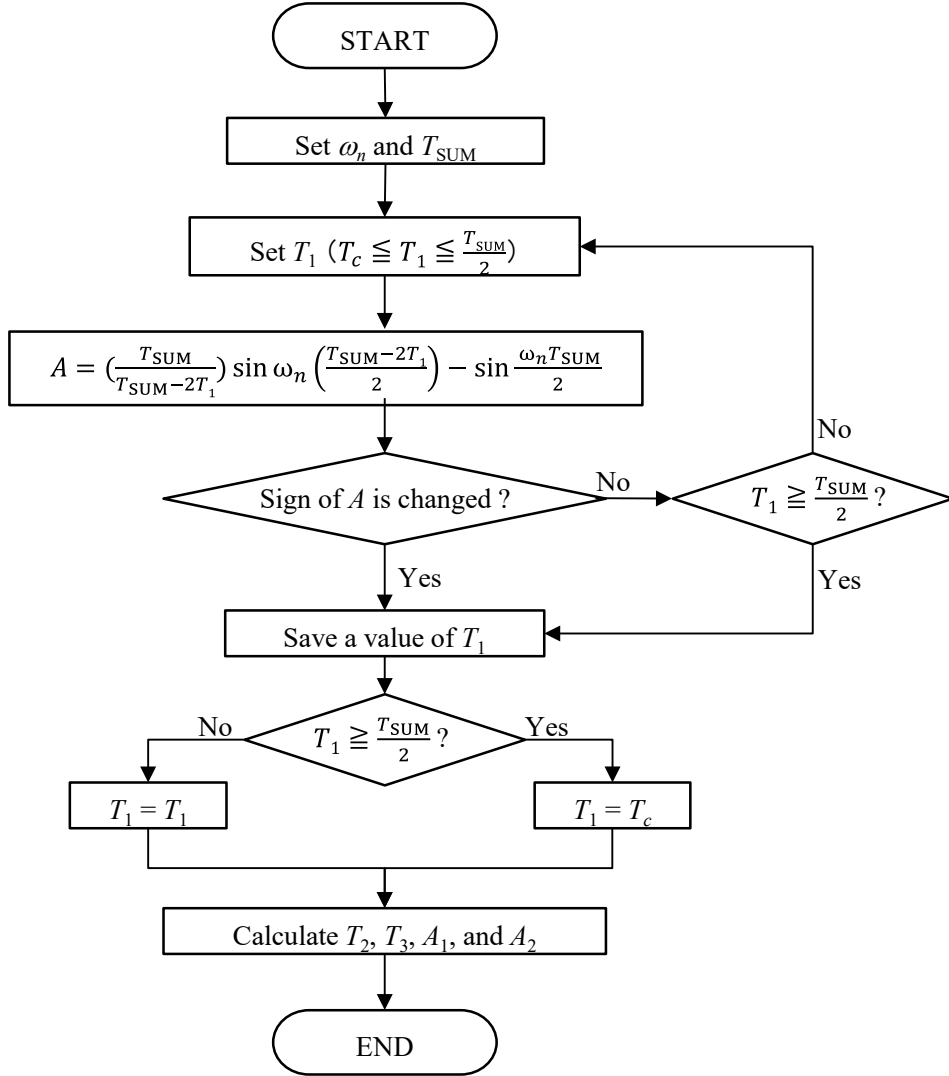


Figure 11: Proposed algorithm for designing acceleration and deceleration processes

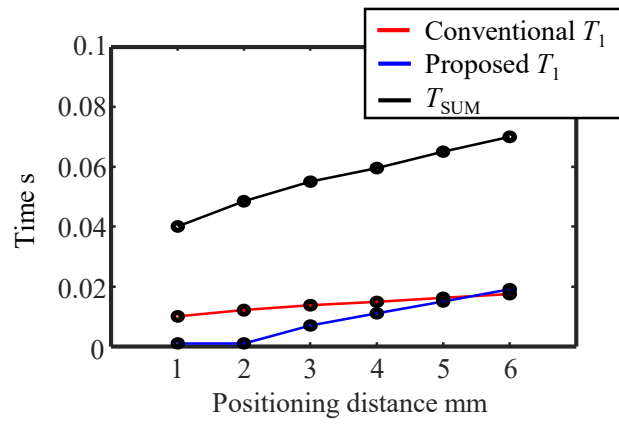
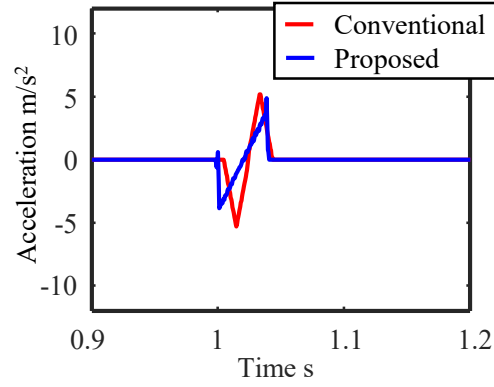
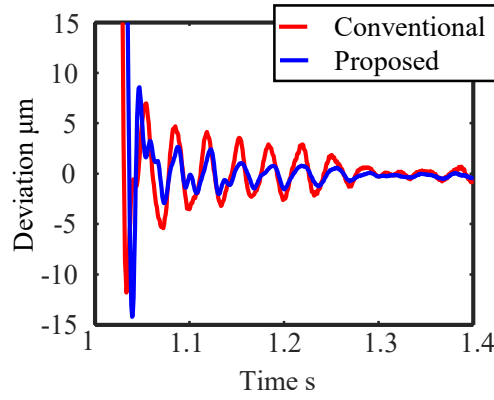


Figure 12: Relationship between positioning distance and designed parameter

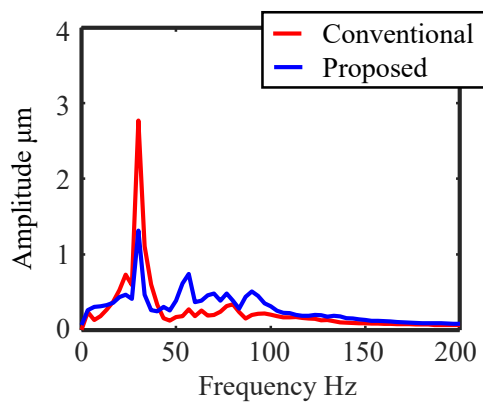




(a) Acceleration profiles

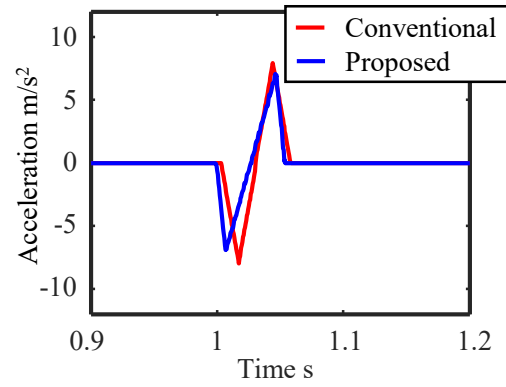


(b) Residual vibrations

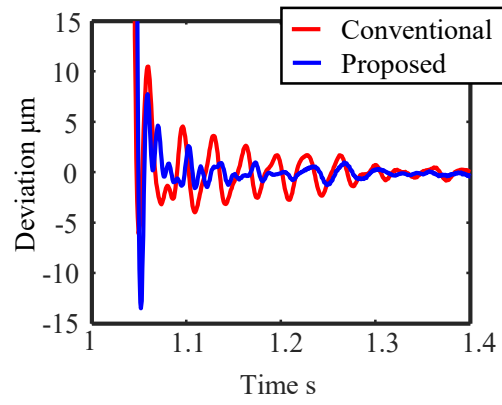


(c) Frequency analysis results

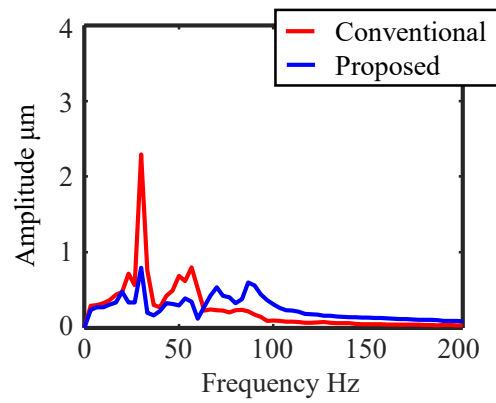
Figure 13: Comparison of measurement results (1 mm distance)



(a) Acceleration profiles



(c) Residual vibrations



(c) Frequency analysis results

Figure 14: Comparison of measurement results (3 mm distance)